Geographic Information System for Soil Erosion Management
Taiyuan, Shanxi Province, China
2-11 June, 1992

SOIL EROSION PREDICTION AND GIS: LINKING THEORY AND PRACTICE

I.D. **Moore**, Canberra, J.P. **Wilson**, Bozeman and
C.A. **Ciesiolka**, Toowoomba

SUMMARY

A simple erosion index is proposed that accounts for the major hydrological and terrain factors affecting erosion. The index is a dimensionless sediment transport capacity that is a non-linear function of specific discharge and slope. It is derived from the transport capacity limiting sediment flux in the Hairsine-Rose, WEPP and catchment evolution erosion theories. For a two-dimensional hillslope, the index is equivalent to the length-slope factor in the Revised Universal Soil Loss Equation, but it is simpler to use and conceptually easier to understand. A major advantage of the index is that it can be easily extended to three-dimensional terrain. It also accounts for different runoff producing mechanisms and soil properties using a spatially variable weighting function and can be implemented within a GIS. Application of the index for erosion potential mapping is demonstrated for the Springvale catchment in Queensland, Australia.

1 INTRODUCTION

Hydrological, erosional and biological processes occurring in landscapes respond primarily to the integrated effects of climate, terrain and substrate (geology). Climate and substrate often have strong linkages to terrain and terrain can, in part, characterize a variety of processes occurring in the landscape as well as many of interrelationships between land, water and vegetation. Several theories and models for examining soil erosion under a variety of data constraints are available in the literature and are described. These range from complex process-based models to simple empirical equations.

In the past we have been able to model specific point and two-dimensional (2-D) (i.e., hillslope) erosional processes in considerable detail, but have not been able to very successfully represent the spatial variability of these processes in real 3-D terrain. We are proposing a simple, topographically-based, erosion index that accounts for the major forcing functions affecting erosion. With the index approach we sacrifice some physical sophistication or rigour to allow more useful estimates of spatial patterns of erosion in landscapes. These topographic indices provide a knowledge-based approach to environmental analysis and can be imbedded within the data analysis subsystems common to most geographic information systems (GISs). This paper only examines the impact of hydrology and terrain on erosion processes acting in landscapes.

2 EROSION THEORY

Here we describe four approaches that represent the "state-of-the-art" in erosion modelling. They range from conventional empirical approaches to sophisticated physically-based or process-oriented models. They also cover simulation time scales ranging from seconds to thousands of years (geological time scales), as well as both dynamic and steady-state models.

2.1 Universal Soil Loss Equation

The Universal Soil Loss Equation (USLE) was empirically derived from over 10,000 plot-years of data (WISCHMEIER & SMITH 1978) and has recently been revised (RENARD et al. 1991). The USLE and the Revised Universal Soil Loss Equation (RUSLE) and can be written as

$$A = R\,K\,LS\,C\,P \qquad (1)$$

where A is the soil loss, R is the rainfall-runoff erosivity factor, K is a soil erodibility factor, L is a slope length factor, S is a slope steepness factor, C is a cover-management factor and P is a supporting factor. Landuse and management are represented by CP and can, with some difficulty, be inferred by remote sensing combined with ground-truthing. Climate erosivity is represented by R and can be computed directly from a knowledge of rainfall intensities and amounts: it varies on a regional scale. Soil erodibility is represented by K, and in the United States values of K have been interpolated or measured for all mapped soil series as part of the Soils-5 database that is derived from County Soil Surveys. Soil series are mapped at scales of 1:15000 to 1:20000 in these surveys. The effects of topography and hydrology on soil loss are characterised by the combined LS factor. Soil loss predictions are more sensitive to slope steepness than slope length. Estimation of the LS factor poses more problems than any of the other factors in the USLE (RENARD et al. 1991) and is a particular problem in applying it to real landscapes as part of a GIS. Table 1 presents expressions for the L and S factors in both the USLE and RUSLE.

There are a number of implicit assumptions concerned with runoff generation and sediment transport imbedded in the equation, including: (1) runoff is generated uniformly over a catchment; (2) runoff occurs via the infiltration excess mechanism (i.e. Hortonian overland flow) and ignores saturation overland flow; and (3) sediment deposition is not represented. These assumptions help to explain why the application of this model to landscapes is so much more difficult than its application to soil loss plots (i.e., uniform slope profiles). The third assumption, in particular, represents a major practical problem because the model does not distinguish those parts of hillslope profiles experiencing net erosion and those areas experiencing net deposition (i.e., the lower ends of concave slopes). The model should only be applied to those parts of the landscape experiencing net erosion (WILSON 1986). GRIFFIN et al. (1988) have rewritten the original USLE to calculate erosion at any point in a landscape experiencing net erosion. Their equation is much easier to implement for large areas although the user must still distinguish those areas experiencing net erosion and deposition at the outset. Their approach can also be combined with the irregular slope adjustment proposed by FOSTER & WISCHMEIER (1974) and used to determine average soil loss along hillslope profiles. Both of these versions retain the 1-D structure of the original equation and as a result, they cannot (like the original model) directly handle converging and diverging terrain i.e., real 3-D landscapes).

2.2 Water Erosion Prediction Project (WEPP) Theory

The United States Department of Agriculture (USDA) is developing improved, process-based erosion-prediction models aimed at replacing the USLE by 1995. WEPP is to be delivered in three versions: profile, watershed and grid, with the profile version being the direct replacement of the USLE (LAFLEN et al. 1991a). WEPP is based on FOSTER et al.'s (1981) concept that divides erosion into an interrill component representing detachment and transport by raindrops and very shallow flows and a rill component that represents net erosion or deposition in rills. Erosion occurring in channels where detachment is due to hydraulic shear is also represented (LAFLEN et al., 1991a). WEPP performs its internal calculations on a per rill area basis.

The theory is encapsulated by the following steady-state sediment continuity equation for a rill:

$$\frac{dq_s}{ds} = D_f + D_i \qquad (2)$$

where q_s is the sediment flux (kg $m^{-1}s^{-1}$), D_i is the interill sediment delivery rate to the rill (kg $m^{-2}s^{-1}$) and D_f is the net erosion or deposition rate in the rill (kg $m^{-2}s^{-1}$) (FOSTER et al. 1989, FOSTER & MEYER 1975). The shallow flow hydraulics in the interrill areas are not directly modelled, but their effects on delivering sediment to the rill are lumped with the rainfall kinetic energy term and modified by a land slope adjustment factor in the expression for D_i, which can be written as:

$$D_i = K_i I_e^2 C_g C_c S_f \left(\frac{R_s}{w}\right) \tag{3}$$

where K_i is the interrill erodibility (kg s m^{-4}), I_e is the effective rainfall (m s^{-1}), C_g is a ground cover adjustment factor, C_c is a canopy cover adjustment factor, S_f is a slope adjustment factor (= 1.05 - 0.85 e^{-4sina}), a is the slope of the land surface towards the rill, R_s is the spacing between rills (m per rill) and w is the rill width (m) (FOSTER et al. 1989, LAFLEN et al. 1991b). The net erosion or deposition rate in the rill, D_f, is

$$D_f = \phi (T - q_s) \tag{4}$$

where T is the sediment transport capacity in the rill (kg $m^{-1}s^{-1}$), $\phi = 0.5\ v_s/q$ for net deposition in the rills (when $T < q_s$) and $\phi = D_c/T$ for net soil detachment in the rills (when $T > q_s$), q is the water flux ($m^3\ m^{-1}s^{-1}$), v_s is the sediment settling velocity (m s^{-1}) and D_c is the detachment capacity of rill flow (kg $m^{-2}s^{-1}$). D_f is positive when there is net erosion and negative when there is net deposition. The detachment capacity of rill flow can be expressed as:

$$D_c = K_r \tau \left(1 - \frac{\tau_o}{\tau}\right) \quad \text{for } \tau > \tau_o \qquad \text{and} \qquad D_c = 0 \quad \text{for } \tau \le \tau_o \tag{5}$$

where τ is the flow shear stress acting on the soil particles (Pa), τ_o is a threshold shear stress (Pa) and K_r is a rill erodibility parameter (s m^{-1}). The sediment transport capacity is represented by an approximation of the Yalin sediment transport equation :

$$T = k_t \tau^{3/2} \tag{6}$$

where k_t is a transport coefficient ($m^{1/2}\ s^2\ kg^{-1/2}$).

2.3 Hairsine-Rose Theory

The Hairsine-Rose theory is a process-based approach that recognizes raindrop impact and surface flow as the agents causing erosion of surface soils. Rainfall detachment, entrainment (detachment by overland flow), rainfall re-detachment and re-entrainment of deposited sediment and deposition are modelled as separate processes (HAIRSINE & ROSE 1991a 1991b 1991c). The theory is an outgrowth of concepts originally developed by ROSE et al. (1983) and ROSE (1985). The theory is encapsulated by the following one-dimensional sediment continuity equation:

$$\frac{\partial q_{si}}{\partial s} + \frac{\partial (C_i h)}{\partial t} = r_i + r_{di} + e_i + e_{di} + r_{gi} - d_i \tag{7}$$

where q_{si} (= qC_i) is the sediment flux (kg $m^{-1}s^{-1}$) in the direction of flow (s), q is the water flux (specific discharge), C_i is the sediment concentration (kg m^{-3}), h is the depth of overland flow (m), r_i, r_{di}, e_i, e_{di} and d_i are the rainfall detachment, rainfall re-detachment, entrainment, re-entrainment and deposition, respectively (kg $m^{-2}s^{-1}$), and subscript i refers to each of N sediment settling velocity classes (i) with an equal mass of soil in each class. The gravity process rate is r_{gi} and represents contributions from headcut collapses and slumping of rill walls (HAIRSINE & ROSE 1991b).

Rainfall detachment, entrainment and deposition can be expressed as follows:

Rainfall Detachment $r_i = (1-H)\, k\, C_e\, i^p/N$ (8a)

$$r_{di} = H\, k_d\, C_e\, i^p\, f_{di} \quad (8b)$$

Entrainment $e_i = (1-H)\,\frac{\eta}{N\,E}\,(\omega - \omega_o)$ for $\omega > \omega_o$ (9a)

$$e_{di} = H\,\eta\,\frac{\alpha_i\, f_{di}}{g}\left(\frac{\rho_s}{\rho_s - \rho}\right)\left(\frac{\omega - \omega_o}{h}\right) \quad \text{for } \omega > \omega_o \quad (9b)$$

Deposition $d_i = \alpha_i\, v_{si}\, C_i$ (10)

where H is the fraction of the soil shielded by a deposited layer, k and k_d are measures of the detachability (kg s m^{-4}) of the original and deposited soil, respectively, C_e is the fraction of soil surface exposed to raindrop impact, i is the rainfall rate (m s^{-1}), p is a nondimensional exponent, f_{di} is the fraction of particles (on a mass basis) in settling velocity class i in the deposited layer, η is the fraction of the available stream power available for entrainment, E is the energy required to entrain a unit mass of soil or specific energy of entrainment (J kg^{-1}), ω is the stream power (watts m^{-2}), ω_o is the threshold stream power, α_i is the ratio of the sediment concentration next to the bed to the mean concentration across the entire depth (C_i) so that $\alpha_i \geq 1$, ρ is the density of the sediment laden water (kg m^{-3}) ($\rho = 1000 + 0.615C$), ρ_s is the density of detached soil or soil aggregates (kg m^{-3}), h is the depth of flow (m), and v_s is the sediment settling velocity (m s^{-1}). The depositabilty of the sediment is equal to $\Sigma v_{si}/N$.

Equations (8) and (9) assume that rainfall detachment and entrainment are nonselective whereas Eq. (10) shows that deposition is highly selective. The re-entrainment process represented by Eq. (9b) assumes that the deposited soil has no cohesive strength. The stream power used in Eqs (9a) and (9b) is the stream power per unit wetted area (RHOADS 1987), $\omega = \rho g q \sin\beta$, where ρg is the unit weight of water and β is the slope of the energy grade line, which is assumed equal to the land slope. An equivalent expression for stream power is $\omega = \tau\, v$, where τ is the shear stress and v is the flow velocity. In Eq. (9b) the ω/h term is equivalent to $\rho g v \sin\beta$, where $v\sin\beta$ is the unit stream power (watt N^{-1} or m s^{-1}), defined as the stream power per unit weight of water. In both Eqs (9a) and (9b) $e_i = 0$ and $e_{di} = 0$ when $\omega \leq \omega_o$. The fraction of available stream power for entrainment (η) is about 0.1, although it increases to 0.2 for low stream powers, and typical values of E in eq. (9a) are 20-30 J kg^{-1} for cultivated soils and 100-150 J kg^{-1} for rangeland soils (HAIRSINE personal communication). Also, the exponent p in Eq. (8a) is usually assumed to to be 1. The soil rainfall detachability terms in Eqs (8a) and (8b) can be written as functions of the maximum detachability (k_o and k_{do}) and water depth (h):

$$k = k_o\left(\frac{h_o}{h}\right)^b \quad \text{for } h > h_o \quad \text{and} \quad k = k_o \quad \text{for } h \leq h_o \quad (11a)$$

$$k_d = k_{do}\left(\frac{h_o}{h}\right)^b \quad \text{for } h > h_o \quad \text{and} \quad k_d = k_{do} \quad \text{for } h \leq h_o \quad (11b)$$

where h_o is a threshold water depth.

2.4 Catchment Evolution Theory: Erosion on Geologic Time Scales

WILLGOOSE et al. (1991) have recently proposed a hillslope and catchment evolution model that explicitly differentiates between the sediment transport behaviour in channels and on hillslopes via coupled flow and sediment continuity equations in the hillslope and channel. Both diffusive (function of slope only, e.g. raindrop splash, soil creep and rock slide) and fluvial (function of slope and discharge) sediment transport processes and tectonic uplift are represented. Channel initiation is

modelled as a threshold process that is nonlinearly related to slope and discharge. The governing sediment continuity equation and channel indicator function can be expressed, respectively, as:

$$\frac{\partial z}{\partial t} = c_o(x,y) + \frac{1}{\rho_s (1-n)}\left(\frac{\partial q_{sx}}{\partial x} + \frac{\partial q_{sy}}{\partial y}\right) + D_z\left(\frac{\partial^2 z}{\partial x^2} + \frac{\partial^2 z}{\partial y^2}\right) \qquad (12a)$$

$$\frac{\partial Y}{\partial t} = d_t\left[0.0025\,\frac{a}{a_t} - 0.1Y + \frac{Y^2}{1+9Y^2}\right] \qquad (12b)$$

where z is elevation, c_o is the rate of tectonic uplift, ρ_s is the density of eroded material, n is the porosity of material before erosion and after deposition, D_z is a diffusivity constant, Y is a channel indicator function (=0 hillslope; = 1 channel; $0 \le Y \le 1$), d_t is a rate constant for channel growth, a is a channel initiation function [$= \varphi_1 q^{m1} (\sin\beta)^{n1}$], a_t is a channel initiation threshold, β is the slope angle in the direction of steepest descent, and φ_1, m1 and n1 are constants. The sediment flux, q_s, is a function of the water flux, q, and the land surface slope, β:

$$q_s = \varphi_2\, q^m\, (\sin\beta)^n \qquad (13)$$

where m and n are constants and φ_2 is a rate constant for sediment transport, that is different for hillslopes and channels. In Eq. (12b) Y=0 for $a<a_t$, goes into a transition when $a=a_t$, increasing to Y=1 at a speed dependent on the channel growth rate constant, d_t, and once it reaches a value of 1 remains there. Most of the hillslope evolution models developed in the last 20 years solve a sediment continuity equation similar to (12a).

2.5 General Sediment Transport Equations

Using dimensional analysis, JULIEN & SIMONS (1985) have shown that most sediment transport equations can be expressed in the following general form:

$$q_s = \varphi_2\, q^m\, (\sin\beta)^n\, i^\delta \left(1 - \frac{\tau_o}{\tau}\right)^\varepsilon \qquad (14)$$

where i is the rainfall intensity, φ_2, n, m, δ and ε are experimental or physically-based coefficients, and the other terms are as previously defined. JULIEN & SIMONS (1985) state that the first three terms (sin β, q, i) represent the potential erosion or transport by flow, which is reduced by the last term (the shear stress term) reflecting the soil resistance to erosion. When τ_o is small compared to τ, the shear stress term can be neglected. The rainfall intensity term is also ignored in many sediment transport equations (i.e., $\delta = 0$), but this is only strictly true for turbulent flows in deep channels.

If we assume rainfall excess is generated uniformly over a catchment then $q = A_s i_e$, where A_s is the upslope contributing area per unit width of contour (or rill) or the specific catchment area ($m^2\ m^{-1}$) and i_e is the rainfall excess rate ($m\ s^{-1}$). For a 2-D hillslope where there is no flow convergence or divergence $A_s = \lambda$, the slope length.

2.6 Transport Limiting Case

For large runoff and erosion events the "transport limiting" case where the sediment flux is limited only by the ability of the flow to carry the sediment is likely to be the dominant influence on the pattern of erosion in landscapes. With the WEPP theory this transport limiting case occurs when q_s = T. We can represent the overland flow hydraulics as uniform turbulent flow using Manning's equation. The WEPP theory assumes that sediment is transported from a site by concentrated flow in rills. By approximating the relationship between hydraulic radius, R, and rill cross sectional area, A, by $R = UA^{1/2}$, where U is a rill shape factor (MOORE & BURCH 1986c), Eq. (6) can be written in

terms of the specific discharge, q (discharge per unit width of catchment, not the discharge per unit width of rill), and slope angle, β:

$$T = q_s = k_t (\rho g)^{1.5} \left(\frac{R_s n}{U^2} \right)^{0.56} q^{0.56} (\sin\beta)^{1.22}$$

$$= k_t (\rho g)^{1.5} \left(\frac{R_s i_e n}{U^2} \right)^{0.56} A_s^{0.56} (\sin\beta)^{1.22} \qquad (15)$$

where n is Manning's roughness coefficient and R_s is the rill spacing (m per rill). If we write Eq. (15) in a dimensionless form so that T*, the dimensionless sediment transport capacity, is unity when $A_s = 22.13$ m^2 m^{-1} and $\tan\beta = 0.09$ (as with the LS factor in the USLE), then:

$$T^* = \left(\frac{A_s}{22.13} \right)^{0.56} \left(\frac{\sin\beta}{0.0896} \right)^{1.22} \qquad (16)$$

where the exponents 0.56 and 1.22 are equivalent to the slope-length and slope-angle exponents, m and n, respectively, in the LS factor in the USLE. If shallow sheet flow were assumed rather than concentrated flow in rills then the exponents in Eq. (16) would be 0.9 and 1.05, respectively.

In the Hairsine-Rose theory the equivalent "transport limiting" case under the steady-state sediment flux occurs when $\partial(C_i h)/\partial t = 0$ and H=1 in Eqs (7) to (10) (HAIRSINE & ROSE, 1991b), which corresponds to the condition where there is a layer of deposited sediment over the entire hillslope. If the threshold term, ω_o/h, in Eq. (9b) is small compared to ω/h, and can therefore be neglected, then the re-entrainment rate given by Eq. (9b) can be rewritten as:

$$e_{di} = H \eta \frac{\rho \alpha_i f_{di}}{n^{0.6}} \left(\frac{\rho_s}{\rho_s - \rho} \right) q^{0.4} (\sin\beta)^{1.3}$$

$$= H \eta \frac{\rho \alpha_i f_{di}}{n^{0.6}} \left(\frac{\rho_s}{\rho_s - \rho} \right) i_e^{0.4} A_s^{0.4} (\sin\beta)^{1.3} \qquad (17)$$

Again, writing Eq. (17) in dimensionless form like Eq. (16), a dimensionless re-entrainment rate, e*, can be derived:

$$e^* = \left(\frac{A_s}{22.13} \right)^{0.4} \left(\frac{\sin\beta}{0.0896} \right)^{1.3} \qquad (18)$$

which is the unit stream power based length-slope factor proposed by MOORE & BURCH (1986b) (table 1).

The dimensionless re-entrainment rate derived from the Hairsine-Rose theory and derived independently by MOORE & BURCH (1986a, 1986b), e*, is compared to the LS factors in the USLE (LS_{USLE}) and RUSLE (LS_{RUSLE}) (Table 1) in figs 1a and 1b, respectively, for the case where $A_s = \lambda$, and λ is the slope-length. There is a strong monotonic function relating LS_{USLE} to e*, with e* < LS_{USLE} for LS_{USLE} values >1.5, which is consistent with the widely held view that the USLE overpredicts LS values at higher slopes and longer slope-lengths. Figure 1b shows that there is considerable scatter in the LS_{RUSLE} versus e* relationship. However, for $A_s=\lambda=22.13$ m^2 m^{-1} (i.e., $A_s/22.13=1$) there is very close agreement, indicating that the theoretical exponent of 1.3 on the slope term of e*, is quite accurate. The best fit between between LS_{RUSLE} and an equation of the form of Eqs (14) and (18) occurs when the area and slope exponents (m and n) are 0.6 and 1.3, respectively (fig. 1c). The results presented in fig. 1 are for A_s and $\lambda<100$, $\tan\beta<0.25$ and the LS and dimensionless sediment transport capacities <5.

Figure 1d shows that there is also good agreement between the dimensionless sediment transport capacity, T*, that is derived from the WEPP theory and LS_{RUSLE}. To a large degree this is expected as the LS factors developed for the RUSLE by McCOOL et al. (1987, 1989) were derived in part by applying the FOSTER &MEYER (1975) theory, which is the basis of the WEPP model. However, Eq. (18) is functionally simpler and easier to use than the LS_{RUSLE} factors.

These results suggest that the combined LS factor in the USLE and RUSLE are measures of the sediment transport capacity of the flow. Furthermore, they show that a sediment transport equation of the form of Eq. (14) or written in dimensionless form as

$$T_c^* = \left(\frac{A_s}{22.13}\right)^m \left(\frac{\sin\beta}{0.0896}\right)^n \tag{19}$$

with m=0.6 (0.4 to 0.6) and n=1.3 (1.2 to 1.3) can be used to map the effects of hydrology, and hence 3-D terrain, on soil erosion in natural landscapes. The A_s term can characterize the effect of converging and diverging terrain on soil erosion, unlike the λ term in the USLE and RUSLE, which is only applicable to 2-D, non-converging and non-diverging hillslopes. In section 4 we will show how these simplifications of the 2-D and 3-D process-based erosion theories can be used to map the susceptibility of landscapes to erosion using GIS.

3 GEOGRAPHIC INFORMATION SYSTEMS FOR EROSION PREDICTION

3.1 General Approach

In developing a GIS for use by soil and water conservation agencies, a digital elevation model (DEM), which is an ordered array of numbers that represent the spatial distribution of elevations in a landscape, and the primary topographic attributes derived from it, constitute a minimum data set. Soils, vegetation and land tenure information are also essential data for many of the sorts of analyses that could be envisaged with such a system. In the United States grid-based DEMs are available on a 30 m square grid for 7.5 minute quadrangle coverage, which is equivalent to the 1:24,000-scale map series quadrangle. A variety of smaller scale DEMs are also available and some of these are described by MOORE et al. (1992). The 30 m DEM has some compatibility with the pixel size of some remote sensing imagery. The USDA-SCS Soils-5 database provides information on the characteristics and interpretive properties of all soil series identified in the United States, including the soil erodibility factor in the USLE. These data are derived from the USDA-SCS County Soil Surveys that are mapped at scales ranging from 1:15,000 to 1:20:000, depending on the age of the survey (MOORE et al. 1992). The spatial resolution of the GIS for application to soil erosion prediction should be equivalent to the 1:10,000 to 1:25,000 scale maps that are often required for site specific analysis and management, and should be compatible with the pixel sizes of remotely sensed data. Smaller scales may be suitable for regional survey. Specific problems in the application of GIS to soil erosion survey at these smaller scales will be discussed later.

In many developing countries there is a general lack of environmental data for planning projects, but the first information obtained is usually a topographic map. From this elevation data, topographic attributes can be calculated and used in the planning of data collection networks (i.e., hydrological monitoring, soil surveys, biological surveys), and in the initial planning of agricultural and forestry developments. As additional environmental data become available, they can be used to provide improved estimates of the terrain-based indices. For example, the susceptibility of the landscape to sheet and rill erosion can initially be estimated using only topographic data. As hydrological and soils information become available, this information can be integrated into the predictions and finally, as information on vegetation and cover is developed, the full USLE or a complete physically-based erosion model, such as the WEPP or Hairsine-Rose models described above, can be used. Hence, we see different layers of data being developed over time with elevation data and the related

topographic attributes constituting a minimum data set. Adoption of this approach by both Australian and international development agencies has the potential for achieving major cost savings, particularly during the critical initial planning and implementation stages of projects.

Topographic attributes can be easily estimated from a digital elevation model using any one of a number of terrain analysis methods. Most GIS are based on a pixel or cellular structure so that grid-based methods of terrain analysis can provide the primary geographic data for them and can be easily integrated within their analysis subsystems. The following section describes a simple, and computationally efficient method of estimating primary terrain attributes from a grid-based DEM. The attributes that can be calculated using this method include elevation, slope, aspect, curvature, catchment area, flow path lengths and others.

3.2 Calculating Topographic Attributes

It is possible to calculate a variety of topographic attributes by applying a second-order, finite-difference scheme centred on the interior node of a moving 3 x 3 square-grid network such as that shown in fig. 2. The maximum slope, β, aspect, profile curvature, plan curvature and total curvature (the Laplacian-∇^2) of the function defining the surface, of the mid-point in the moving grid can then be calculated. For example, the slope, β, is computed as:

$$\beta = \arctan\left\{\left[\left(\frac{\partial z}{\partial x}\right)^2 + \left(\frac{\partial z}{\partial y}\right)^2\right]^{1/2}\right\} \qquad (20)$$

where

$$\frac{\partial z}{\partial x} = (Z_6 - Z_4)/2\zeta \qquad \text{and} \qquad \frac{\partial z}{\partial y} = (Z_2 - Z_8)/2\zeta \qquad (21)$$

the Z's are the elevations of the nine nodes shown in fig. 2 and ζ is the grid-spacing. Expressions for the other topographic attributes are given in MOORE et al. (1991).

The plan area in the horizontal plane characterised by each node or grid-point is $A_h=\zeta^2$. JENSON & DOMINGUE (1988) describe a computationally efficient algorithm for estimating flow directions and hence catchment areas and drainage path lengths for each node in a regular grid DEM based on the concept of a depressionless DEM. They use the flow direction algorithm developed by O'CALLAGHAN & MARK (1984) which assumes that water flows from a given node to one of eight possible neighbouring nodes, based on the direction of steepest descent - D8 algorithm. Recently, FAIRFIELD & LAYMARIE (1991) modified this algorithm to include a stochastic component when the D8 algorithm computes flow directions in N-E, S-E, S-W and N-W directions - Rho8 algorithm. FREEMAN (1991) and QUINN et al. (1991) have also proposed algorithms that allow flow to be distributed to multiple nearest neighbour elements using a slope-weighting function, thus allowing flow divergence to be represented and overcoming one of the major limitations of grid-based methods of terrain analysis. We have adapted these algorithms to allow flow spreading above defined channels and either the D8 or Rho8 algorithm below points of channel initiation - FD8 and FRho8 algorithms, respectively. This algorithm can be combined with the above finite-difference approach to estimate a wide variety of topographic attributes that are important in erosion and hydrologic analyses.

4 EROSION PROCESS PREDICTION IN COMPLEX TERRAIN

The data analysis subsystem is potentially the most powerful component of a GIS, but is often the most under-utilised. Erosion models can be imbedded within such a GIS subsystem or the model can be linked to the data input and output subsystems and run outside the GIS. Both approaches can provide efficient methods of interpreting landscape behaviour from primary geographic data. Most of the attempts to date have utilized the second approach in conjunction with the USLE without addressing the problems that are incurred in scaling up USLE applications from slope profiles to

large areas (i.e., catchments, counties, etc.). Descriptions of GIS/USLE applications by VENTURA et al. (1988) and HESSION & SHANHOLTZ (1988), for example, fail to mention the need to distinguish areas experiencing net erosion and net deposition before applying this equation (as discussed earlier). It is not clear how they respond to this challenge (if at all) and the discussion about scale (i.e., the size of the raster cells and/or vector polygons used to compute soil loss) and the consequences of using source data compiled at different scales is also vague. Hence, the definition of slope gradient and length used by VENTURA et al. (1988) is unclear and the definitions used in both applications are probably different from those specified in the original USLE. The data could have been compiled, interpreted and used in conjunction with the USLE in ways that avoided these problems (see GRIFFIN et al. 1988). We have chosen a different approach here that avoids these kinds of problems and limitations of a one-dimensional model such as the USLE. The spatial distribution of erosion potential is mapped with the simple dimensionless sediment transport index given by Eq. (19). This index provides a means of identifying areas in a catchment that are highly susceptible to erosion and where erosion mitigation works might be successfully targeted.

The 9.6 ha Springvale catchment located in central Queensland, Australia is used to demonstrate the method. In 1979 the catchment was highly degraded due to overgrazing, at which time improved vegetation and cattle management practices were implemented in an attempt to rehabilitate the catchment. The Springvale catchment has been monitored since 1979, and there are good records of geology, soil types and their physical properties, vegetation distribution (at various times), precipitation and runoff records, and detailed 1 m contour interval elevation data (CIESIOLKA 1987). Here, we only used the elevation and soils data to create a series of GIS data layers using a 25 m^2 grid-cell size. The GIS contained the following attributes at each grid-cell: elevation, slope, aspect, plan curvature, profile curvature, soil type, steady-state infiltration rate (measured using small rainfall simulators), and three different measures of specific catchment area that are described below. The effect of spatially variable vegetation on erosion is not considered here because of space limitations.

The specific area, A_s in Eq. (19), can be rewritten to account for varying runoff generation in each cell to give a more general form of the dimensionless sediment transport capacity equation:

$$T_{cj}^* = \left(\frac{\sum_{i=1}^{j} (\mu_i \, a_i)/b_j}{22.13} \right)^m \left(\frac{\sin\beta_j}{0.0896} \right)^n \qquad (22)$$

where μ_i is a weighting coefficient ($0 \le \mu_i \le 1$) that is dependent on the runoff generation mechanism and soil properties (i.e., infiltration rates), a_i is the area of the ith cell (25 m^2), b is the width of each cell, and i=1,j represents all of the i cells hydraulically connected to cell j. When μ=0 no rainfall excess is generated; when μ=1 100% rainfall excess is generated.

Three cases are considered: (1) $\mu_i=\mu=1$, which assumes that rainfall excess is generated uniformly over the entire catchment; (2) Hortonian overland flow in which μ_i is spatially variable and a function of the infiltration characteristics of the soil; and (3) saturation overland flow in which overland flow only occurs in zones of saturation in the landscapes. For case (3) $\mu_i=0$ when $\ln(A_s/\tan\beta)<W_c$ and $\mu_i=1.0$ when $\ln(A_s/\tan\beta)\ge W_c$, where $\ln(A_s/\tan\beta)$ is a wetness index (MOORE et al. 1988) and W_c is a critical wetness index that identifies the location of zones of surface saturation in the landscape. The predicted dimensionless sediment transport capacities, T_c^*, for these three cases are presented in figs. 3a, 3b, and 3c, respectively. In case (3) a critical wetness index of 6.0 was somewhat arbitrarily selected. In all cases m=0.6 and n=1.3 were assumed. Zones with $T_c^*>2.5$ in fig. 3b show good agreement with areas of degradation observed in the catchment in 1979 and 1980 when vegetation was sparse. The cumulative frequency distributions of the predicted sediment transport capacity indices for the three cases are presented in fig. 4.

The change in sediment transport capacity across a grid-cell, ΔT_c, provides a possible measure of the erosion or deposition potential in each cell (MOORE & BURCH 1986a). Conceptually, ΔT_c is

related to the dq_s/ds term in Eqs. 2, 7 and 12a when the sediment transport limiting case is considered (i.e., when $q_s = T_c$). The change in sediment transport capacity can be written as:

$$\Delta T_{cj} = \varphi \left[A_{sj-}^{m} (\sin\beta_{j-})^{n} - A_{sj}^{m} (\sin\beta_{j})^{n}\right] \qquad (23)$$

where φ is a constant, subscript j signifies the outlet of cell j and j- signifies the inlet to cell j. The specific catchment areas, A_s, can also be written in terms of weighting coefficients and cell areas, as in Eq. 22. A positive value of ΔT_{cj} indicates net deposition and a negative value indicates net erosion. The predicted distribution of the potential erosion and deposition index, $\Delta T_c/\varphi$, is shown in fig. 5 for which a uniform rainfall excess was assumed (μ_i=μ=1). Above the main channel lines this relationship is well behaved and indicates a general erosional landscape. Near the main stem of the channel system waves of erosion and deposition are predicted. It is not yet possible to determine if this is a real phenomenon or an artifact of the method of analysis but some general observations can be made. Sediment pulses in the form of lag deposits (course sediment deposited in elongated bars about 0.5 m long and 0.2 m wide after storm events) have been observed in the valley floor, but appear to be more widely spaced than predicted by fig. 5. Also, the areas of predicted deposition do coincide with the location of alluvial fans in some cases.

The erosion models discussed here lack the capacity to describe gully incision and headwall retreat across a slope. The Springvale catchment is at that geomorphological stage when headwall retreat is occurring and subsurface flow appears to be playing a role in this retreat. Case (3), described above and presented in fig. 3c, maps the zones of surface saturation and hence can define the upslope limits on potential exfiltration in the catchment using the critical wetness index approach. However, the model does not yet represent the erosional processes caused by this exfiltration. A terrain analysis-based approach using observed slope-upslope contributing area relationships for channel initiation appears to offer a means for characterizing headwall retreat.

The results shown in figs. 3 and 5 demonstrate that erosion and deposition processes are highly variable over length scales of 5-20 m to 100-200 m. Therefore, if GIS is to be used to map erosion and deposition using primary landscape, soil and vegetation attributes the grid- or raster-size of the GIS must be capable of capturing small-scale variations in slope and specific drainage area in particular. In the example presented here we used a grid-spacing of 5 m, but in other applications we have successfully applied similar methods up to grid-spacings of about 20 m. There are important scale related issues concerned with the estimation of slope, specific catchment area and flow path length within a GIS for erosion modelling. Some of these issues have been discussed by MOORE et al. (1992) and are not repeated here. It appears that cell sizes need to be small in order to characterize landscape erosion and deposition.

If the grid-spacing of a GIS is on the order of 100 m or greater then it is not possible to use the GIS to model erosion using this process-based approach and primary landscape attributes. Rather, erosion and deposition in an individual raster cell can only be realistically represented as a distribution function similar to those shown in fig. 4. These sigmoid distribution functions can be represented by three-parameter gamma distributions. It is probably more realistic to store the values of these three parameters as data layers within the GIS.

5 CONCLUSIONS

By considering the transport limiting entrainment rate (H=1) in the steady-state version of the Hairsine-Rose erosion theory, the sediment transport limiting case in the WEPP theory and the general forms of the sediment flux expressions in a model of catchment evolution, a dimensionless sediment transport capacity index can be derived. It provides a powerful tool for identifying areas within a catchment that are highly susceptible to erosion and where erosion mitigation works might be successfully targeted. For a two-dimensional hillslope, the index is equivalent to the combined length-slope factor (LS) in the Revised Universal Soil Loss Equation, but it is simpler to use and conceptually easier to understand. The Revised Universal Soil Loss Equation provides lower estimates of the LS factor for longer slope-lengths and steeper slope-angles than in the original

Universal Soil Loss Equation. These results lend support to the concept of the LS factor as a measure of the sediment transport capacity of overland flow.

A major advantage of the index is that it can be easily extended to three-dimensional terrain. The specific discharge is a function of the specific drainage area, soil properties and rainfall intensity. Therefore, the index can be estimated as a function of primary terrain attributes and soil properties and can be readily implemented within an appropriately scaled GIS. The index was used to successfully map the highly degraded areas of the 9.6 ha Springvale catchment in Queensland, Australia.

ACKNOWLEDGEMENTS

This study was funded in part by grant No. 90/6334 from the Bilateral Science and Technology Program of the Department of Industry, Technology and Commerce (Australia), grants SES-8912042 and SES-8912938 from the National Science Foundation (USA) and by the Water Research Foundation of Australia. The authors wish to thank Dr. Mike Hutchinson, Centre for Resource and Environmental Studies, Australian National University for the use of program ANUDEM, with which we developed the 5 m grid digital elevation model of the Springvale catchment and Mr. Robin Connolly, Mr. Mark Silburn and the officers of the Land Management Research Branch, Queensland Department of Primary Industry for the infiltration data from the Springvale catchment that were used to demonstrate the technology described in this study.

REFERENCES

[CIESIOLKA 1987] Ciesiolka, C.: Catchment management in the Nogoa watershed. Australian Water Resources Council Research Report 80/128, Canberra, Australia.

[FAIRFIELD & LEYMARIE 1991] Fairfield, J. & Leymarie, P.: Drainage networks from grid digital elevation models. Water Resources Research **27**, 709-717.

[FOSTER & MEYER 1975] Foster, G.R. & Meyer, L.D.: Mathematical simulation of upland erosion using fundamental erosion mechanics. Proceedings of the Sediment Yield Workshop, United States Sedimentation laboratory, Oxford, Mississippi, RS-S-40, 190-201.

[FOSTER et al. 1989] Foster, G.R., Lane, L.J., Nearing, M.A., Finkner, S.C. & Flanagan, D.C.: Erosion component. USDA-Water Erosion Prediction Project: Hillslope Profile Model Documentation, L.J. Lane and M.A. Nearing (eds). NSERL Report. No. 2, National Soil Erosion Research Laboratory, Agricultural Research Service, United States Department of Agriculture, West Lafayette, Indiana, 10.1-10.12.

[FOSTER et al. 1981] Foster, G.R., Lane, L.J., Nowlin, J.D., Laflen, J.M. & Young, R.A.: Estimating erosion and sediment yield on field size areas. Transactions of the ASAE **24**, 253-262.

[FOSTER & WISCHMEIER 1974] Foster, G.R. & Wischmeier, W.H.: Evaluating irregular slopes for soil loss prediction. Transactions of the ASAE **17**, 305-309.

[FREEMAN 1991] Freeman, T.G.: Calculating catchment area with divergent flow based on a regular grid. Computers & Geoscience **17**, 413-422.

[GRIFFIN et al. 1988] Griffin, M.L., Beasley, D.B., Fletcher, J.J. & Foster, G.R.: Estimating soil loss on topographically nonuniform field and farm units. Journal of Soil and Water Conservation **43**, 326-331.

[HAIRSINE & ROSE 1991a] Hairsine, P.B. & Rose, C.W.: Rainfall detachment and deposition: Sediment transport in the absence of flow-driven processes. Soil Science Society of America Journal **55**, 320-324.

[HAIRSINE & ROSE 1991b] Hairsine, P.B. & Rose, C.W.: Modelling water erosion due to overland flow using physical principles: I. Uniform flow. Water Resources Research **27**, (in press).

[HAIRSINE & ROSE 1991c] Hairsine, P.B. & Rose, C.W.: Modelling water erosion due to overland flow using physical principles: II. Rill flow. Water Resources Research **27**, (in press).

[HESION & SHANHOLTZ 1988] Hession, W.C. & Shanholtz, V.O.: A geographic information system for targeting nonpoint-source agricultural pollution. Journal of Soil and Water Conservation **43**, 264-266.

[JENSON & DOMINGUE 1988] Jenson, S.K. & Domingue, J.O.: Extracting topographic structure from digital elevation data for geographic information system analysis. Photogrammetric Engineering and Remote Sensing **54**, 1593-1600.

[JULIEN & SIMONS 1985] Julien, P.Y. & Simons, D.B.: Sediment transport capacity of overland flow. Transactions of the ASAE **28**, 755-762.

[LAFLEN et al. 1991a] Laflen, J.M., Lane, L.J., & Foster, G.R.: WEPP: A new generation of erosion prediction technology. Journal of Soil and Water Conservation **46**, 34-38.

[LAFLEN et al. 1991b] Laflen, J.M., Elliot, W.J., Simanton, J.R., Holzhey, C.S. & Kohl, K.D.: WEPP: Soil erodibility experiments for rangeland and cropland soils. Journal of Soil and Water Conservation **46**, 39-44.

[McCOOL et al. 1987] McCool, D.K., Brown, L.C., Foster, G.R., Mutchler, C.K. & Meyer, L.D.: Revised slope steepness factor for the Universal Soil Loss Equation. Transactions of the ASAE **30**, 1387-1396.

[McCOOL et al. 1989] McCool, D.K., Foster, G.R., Mutchler, C.K. & Meyer, L.D.: Revised slope length factor in the Universal Soil Loss Equation. Transactions of the ASAE **30**, 1571-1576.

[MOORE & BURCH 1986a] Moore, I.D. & Burch, G.J.: Modelling erosion and deposition: topographic effects. Transactions of the ASAE **29**, 1624-1630, 1640.

[MOORE & BURCH 1986b] Moore, I.D. & Burch, G.J.: Physical basis of the length-slope factor in the Universal Soil Loss Equation. Soil Science Society of America Journal **50**, 1294-1298.

[MOORE & BURCH 1986c] Moore, I.D. & Burch, G.J.: Sediment transport capacity of sheet and rill flow: Application of unit stream power theory. Water Resources Research **22**, 1350-1360.

[MOORE et al. 1988] Moore, I.D., Burch, G.J. & Mackenzie, D.H.: Topographic effects on the distribution of surface soil water and the location of ephemeral gullies. Transactions of the ASAE **31**, 1098-1107.

[MOORE et al. 1991] Moore, I.D., Grayson, R.B. & Ladson, A.R.: Digital terrain modelling: a review of hydrological, geomorphological, and biological applications. Hydrological Processes **5**, 3-30.

[MOORE et al. 1992] Moore, I.D., Turner, A.K., Wilson, J.P., Jenson, S.K. & Band, L.E.: GIS and land surface-subsurface process modelling. Geographic Information Systems and Environmental Modeling

[O'CALLAGHAN & MARK 1984] O'Callaghan, J.F. & Mark, D.M.: The extraction of drainage networks from digital elevation data. Computer Vision, Graphics and Image Processing **28**, 323-344.

[QUINN et al. 1991] Quinn, P., Beven, K., Chevallier, P. & Planchon, O.: The prediction of hillslope flow paths for distributed hydrological modelling using digital terrain models. Hydrological Processes **5**, 59-79.

[RENARD et al. 1991] Renard, K.G., Foster, G.R., Weesies, G.A. & Porter, J.P.: RUSLE Revised universal soil loss equation. Journal of Soil and Water Conservation **46**, 30-33.

[RHOADS 1987] Rhoads, B.L.: Stream power terminology. Professional Geographer **39**, 189-195.

[ROSE 1985] Rose, C.W.: Developments in soil erosion and deposition models. Advances in Soil Science **2**, 1-63.

[ROSE et al. 1983] Rose, C.W., Williams, J.R., Sander, G.C. & Barry, D.A.: A mathematical model of soil erosion and deposition processes. I. Theory for a plane land element. Soil Science Society of America Journal **47**, 991-995.

[VENTURA et al. 1988] Ventura, S.J., Chrisman, N.R., Conners, K. Gurda, R.F. & Martin R.W.: A land information system for soil erosion control planning. Journal of Soil and Water Conservation **43**, 230-233.

[WILLGOOSE et al. 1991] Willgoose, G., Bras, R.L. & Rodriguez-Iturbe, I.: A coupled channel network growth and hillslope evolution model. 1. Theory. Water Resources Research **27**, 1671-1684.

[WILSON 1986] Wilson, J.P.: Estimating the topographic factor in the universal soil loss equation for watersheds. Journal of Soil and Water Conservation **41**, 179-184.

[WISCHMEIER & SMITH 1978] Wischmeier, W.H. & Smith, D.D.: Predicting rainfall erosion losses, a guide to conservation planning. Agriculture Handbook No. 537, United States Department of Agriculture, Washington D.C.

Address of authors:
I.D. Moore
Centre for Resource and Environmental Studies
The Australian National University
GPO Box 4, Canberra, ACT, Australia 2601
J.P. Wilson
Department of Earth Sciences
Geographic Information and Analysis Center
Montana State University
Bozeman, Montana, U.S.A., 59717
C.A. Ciesiolka
Land Management Research Branch
Department of primary Industries
PO Box 102, Toowoomba, Queensland, Australia 4350

Table 1 *LS factors in the Universal Soil Loss Equation (USLE) and Revised Universal Soil Loss Equation (λ=slope length in metres; β=slope angle in degrees).*

	S		L=$(\lambda/22.13)^m$	
USLE (WISCHMEIER & SMITH, 1978)	$65.4\sin^2\beta+4.56\sin\beta+0.0654$		m=0.5 m=0.4 m=0.3 m=0.2	$\tan\beta>0.05$ $0.03<\tan\beta\leq0.05$ $0.01<\tan\beta\leq0.03$ $\tan\beta\leq0.01$
RUSLE	$10.8\sin\beta+0.03$	$\tan\beta<0.09$	$m=F/(1+F)$	
(McCOOL et al. 1987, 1989)	$16.8\sin\beta-0.50$	$\tan\beta\geq0.09$	$F=(\sin\beta/0.0896)/(3\sin^{0.8}\beta+0.56)$*	
	$3\sin^{0.8}\beta+0.56$	$\lambda\leq4$ m	$F=0$	deposition
	$(\sin\beta/0.0896)^{0.6}$	thawing soils with $\tan\beta\geq0.09$	$\lambda=4$ m	$\lambda\leq4$ m
MOORE & BURCH # (1986a, 1986b)	$LS=(A_s/22.13)^m(\sin\beta/0.0896)^n$ where m=0.4, n=1.3, and A_s = specific catchment area			

* Assumes rill and interrill erosion are equal.
\# Derived from unit stream power theory.

Figure Captions

Figure 1: *Comparison of different forms of the dimensionless sediment transport capacity index versus the length-slope factors in the Universal Soil Loss Equation (USLE) and Revised Universal Soil Loss Equation (RUSLE): a) Hairsine-Rose theory-based index versus LS_{USLE}; b) Hairsine-Rose theory-based index versus LS_{RUSLE} (λ = slope length in m); c) WEPP theory-based index versus LS_{RUSLE}; and d) Generalized dimensionless sediment transport equation with m=0.6 and n=1.3 (Eq. 19) versus LS_{RUSLE}.*

Figure 2: *Square-grid network showing a moving 3 x 3 submatrix centred on node 5.*

Figure 3: *Computed spatial distribution of the dimensionless sediment transport capacity index, T_c*, for: a) Spatially uniform rainfall excess; b) Spatially non-uniform rainfall excess generated by Hortonian overland flow; and c) Spatially non-uniform rainfall excess generated by saturation overland flow (W_c=6.0).*

Figure 4: *Cumulative frequency distributions of the dimensionless sediment transport capacity index, T_c*, for: a) Spatially uniform rainfall excess; b) Spatially non-uniform rainfall excess generated by Hortonian overland flow; and c) Spatially non-uniform rainfall excess generated by saturation overland flow (W_c=6.0).*

Figure 5: *Spatial distribution of the erosion and deposition index ΔT_c in which erosion is negative and deposition is positive.*

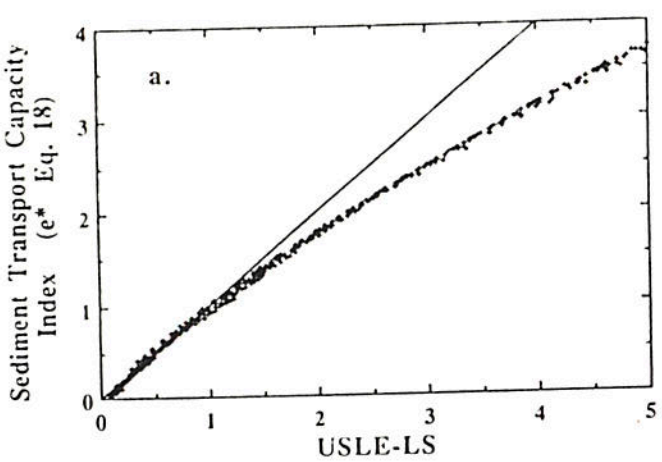
a.
Sediment Transport Capacity Index (e* Eq. 18)
USLE-LS
0
1
2
3
4
5

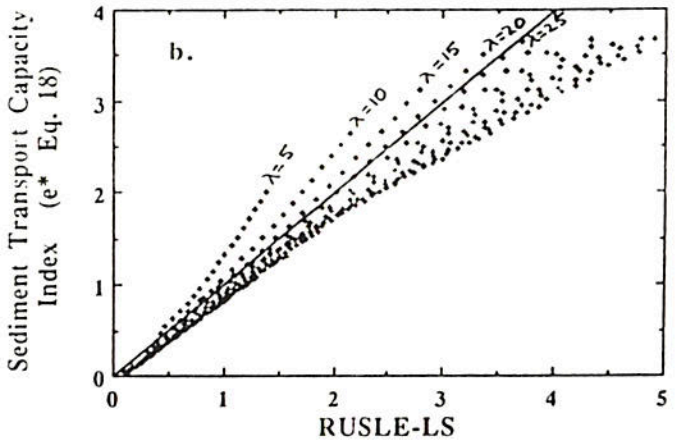
b.
Sediment Transport Capacity Index (e* Eq. 18)
RUSLE-LS
λ=5
λ=10
λ=15
λ=20
λ=25
0
1
2
3
4
5

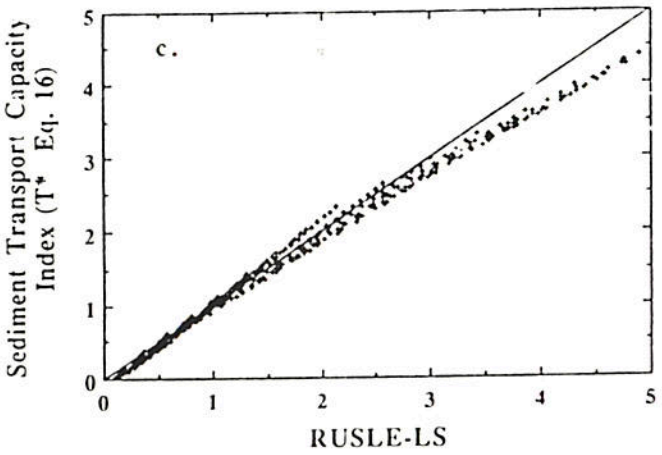
c.
Sediment Transport Capacity Index (T* Eq. 16)
RUSLE-LS
0
1
2
3
4
5

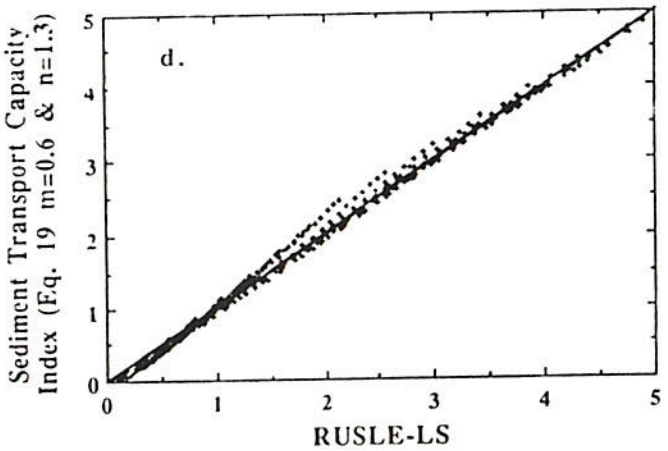
d.
Sediment Transport Capacity Index (Eq. 19 m=0.6 & n=1.3)
RUSLE-LS
0
1
2
3
4
5

Figure 1

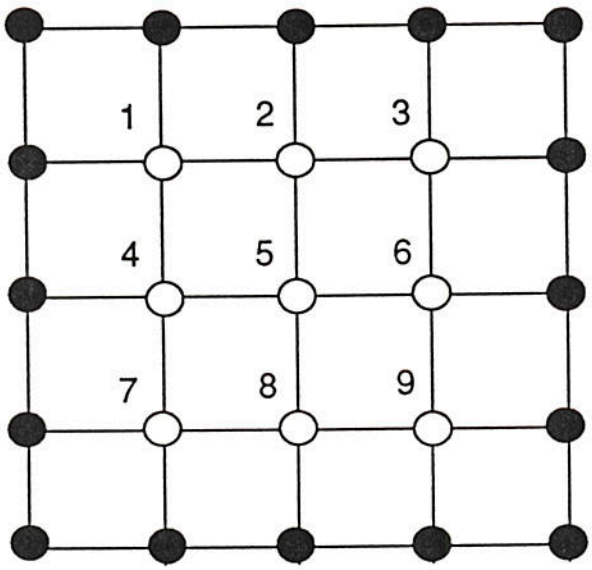

Figure 2

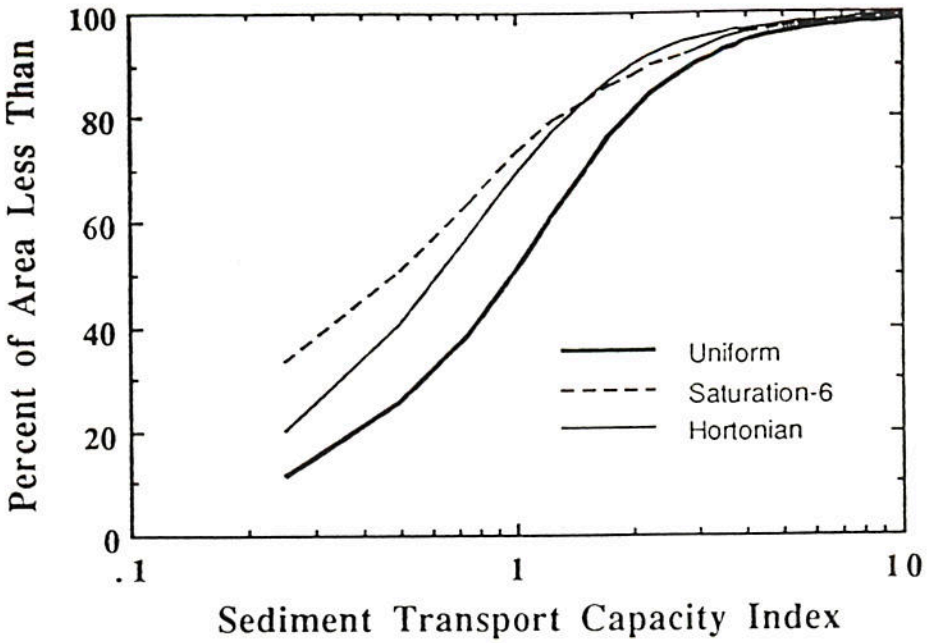

Figure 4

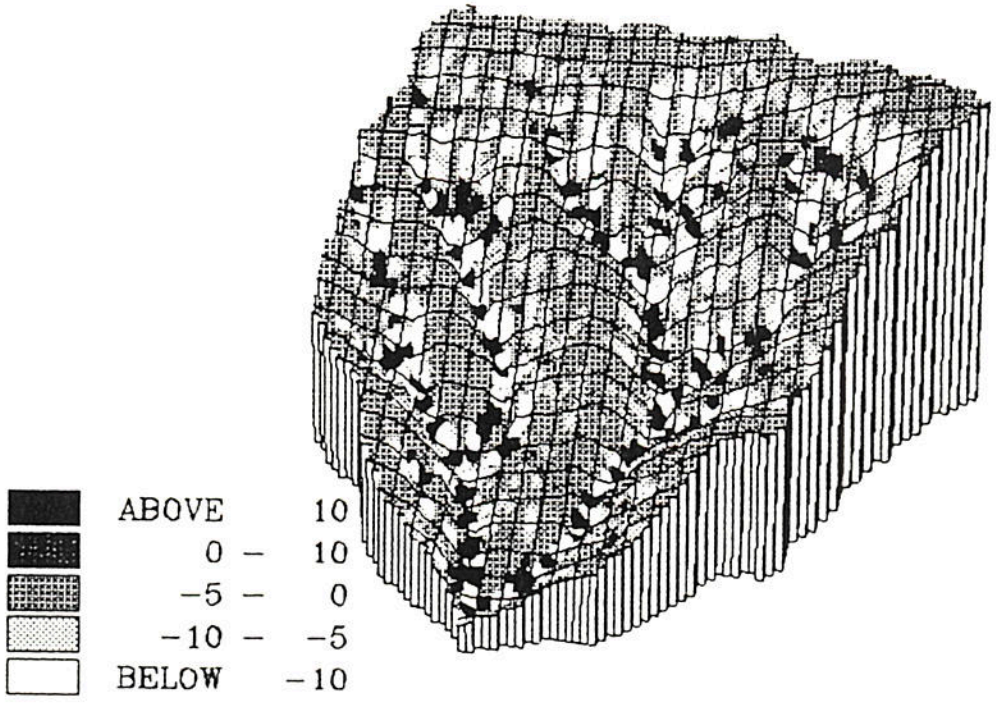

Figure 5

Figure 3